Food & Function

ROYAL SOCIETY OF CHEMISTRY

PAPER

View Article Online
View Journal | View Issue

Cite this: *Food Funct.*, 2024, **15**, 647

Combination of *Lacticaseibacillus paracasei* BEPC22 and *Lactiplantibacillus plantarum* BELP53 attenuates fat accumulation and alters the metabolome and gut microbiota in mice with high-fat diet-induced obesity†

Na-Rae Lee, ‡[a] Tae-Jun Kwon,‡[b] Eui-Chun Chung,‡[c] Jaewoong Bae,‡[c] Song-Hui Soung,[d] Hyun-Ji Tak,[d] Jun-Young Choi,[b] Young-Eun Lee,[e] Nak Won Hwang,[c] Jong Seo Lee,[c] Kum-Joo Shin,[c] Choong Hwan Lee,[a,d] KilSoo Kim*[b,f] and Seokjin Kim *[c]

This study evaluated the effects of formulations with *Lacticaseibacillus paracasei* BEPC22 and *Lactiplantibacillus plantarum* BELP53 on adiposity, the alteration of microbiota, and the metabolome in high-fat diet-fed mice. The strains were selected based on their fat and glucose absorption inhibitory activities and potential metabolic interactions. The optimal ratio of the two strains in the probiotic formulation was determined based on their adipocyte differentiation inhibitory activities. Treatment of formulations with BEPC22 and BELP53 for 10 weeks decreased body weight gain at 6 weeks; it also decreased the food efficiency ratio, white adipose tissue volume, and adipocyte size. Moreover, it decreased the expression of the lipogenic gene *Ppar-γ* in the liver, while significantly increasing the expression of the fat oxidation gene *Ppar-α* in the white adipose tissue. Notably, treatment with a combination of the two strains significantly reduced the plasma levels of the obesity hormone leptin and altered the microbiota and metabolome. The omics data also indicated the alteration of anti-obesity microbes and metabolites such as *Akkermansia* and indolelactic acid, respectively. These findings suggest that treatment with a combination of BEPC22 and BELP53 exerts synergistic beneficial effects against obesity.

Received 25th August 2023,
Accepted 27th November 2023

DOI: 10.1039/d3fo03557c

rsc.li/food-function

Introduction

Obesity is a major global health issue that is associated with several diseases, including diabetes, and some types of cancer.[1] Hormonal and medical treatments for obesity may lack long-term sustainability in terms of their effectiveness and potential adverse effects.[2] Therefore, numerous research groups have endeavoured to develop effective anti-obesity treatments with few side effects.

Probiotics are known to confer health benefits without adverse side effects when consumed in adequate amounts. Some probiotics exhibit anti-obesity effects by regulating glucose and lipid metabolism.[3] In particular, *Lactobacillus* species (*e.g. L. rhamnosus*, *L. brevis*, *L. plantarum*, and *L. paracasei*) lower lipid levels, reduce body weight, and increase glucose and lipid metabolism by modulating the production of hormones and expression of genes related to obesity and inhibiting adipogenesis.[4] Other anti-obesity mechanisms of probiotics include the augmentation of short-chain fatty acid production and modulation of bile acid metabolism.[5] However, such functions of probiotics are strain specific; thus, combining multiple strains may result in symbiotic and synergistic effects.[6] Many probiotics are composed of multiple strains because they are more effective than those composed of individual strains.[2,7]

The gut microbiota plays diverse roles in obesity, from influencing lipid metabolism to modulating appetite.[8–11] The

[a]*Research Institute for Bioactive-Metabolome Network, Konkuk University, Seoul 05029, Republic of Korea*
[b]*Preclinical Research Center, Daegu-Gyeongbuk Medical Innovation Foundation (K-MEDI Hub), Daegu 41061, Republic of Korea. E-mail: kslac@kmedihub.re.kr*
[c]*R&D Center, Hecto Healthcare Co., Ltd, Seoul 06142, Republic of Korea. E-mail: jinkim@hetco.co.kr*
[d]*Department of Bioscience and Biotechnology, Konkuk University, Seoul 05209, Republic of Korea*
[e]*Cognitive Science Research Group, Korea Brain Research Institute Daegu 41062, Republic of Korea*
[f]*College of Veterinary Medicine, Kyungpook National University, 80 Daehakro, Buk-gu, Daegu 41566, Korea*
†Electronic supplementary information (ESI) available. See DOI: https://doi.org/10.1039/d3fo03557c
‡These authors contributed equally to this work.

composition and biodiversity of the gut microbiome significantly differ between individuals with and without obesity.[12–14] The Firmicutes/Bacteroidetes (F/B) ratio, which is positively correlated with the BMI, is high in patients with obesity, but treatment with *Lacticaseibacillus* probiotics can decrease the F/B ratio, as well as the lipoprotein cholesterol levels and body weight.[15,16] The gut microbiome plays a vital role in obesity and is linked to alterations in constituent metabolites during obesity progression.[17]

Therefore, in this study, we paired two strains selected through *in vitro* assays and metabolic characterisation to maximise their anti-obesity effects. Then, we evaluated the anti-obesity activity of the probiotic pair in a high-fat diet (HFD)-induced obese mouse model and analysed its effect on the microbiome and metabolome.

Materials and methods

Isolation and identification of lactic acid bacteria (LAB)

This study was approved by the Public Institutional Review Board designated by the Ministry of Health and Welfare (IRB number: P01-201712-33-002). Human-derived sampling was conducted in accordance with the protocols approved by the Korea's Bioethics and Safety Act no. 16372. All subjects provided written informed consent. Samples of healthy lean adult and infant faeces, raw milk, and kimchi were collected to isolate LAB strains. The samples were mixed with 0.85% NaCl saline for 10 min and then streaked onto De Man–Rogosa–Sharpe (MRS) (Difco-BD, Sparks, MD, USA) agar. The agar plates were incubated anaerobically at 37 °C for 48–72 h. For identification, representative colonies were isolated from plates and inoculated into fresh MRS broth. The isolates were characterised through Gram staining and then subjected to biochemical identification using an API 50 CHL kit (BioMérieux, Marcy, Lyon, France) and 16S ribosomal RNA (rRNA) gene sequencing. For the latter, DNA was extracted using a commercial G-spin kit from each strain (Intron, Gyeonggi, Korea), and the genes were amplified by PCR using the following universal primers: 27F (5′-GAGTTGGATCCTGGCTCAG-3′) and 1492R (5′-AAGGAGGGGATCCAGCC-3′). The isolates were identified through 16S rRNA gene sequence homology analysis using the GenBank database (NCBI, Bethesda, MD, USA).

Bacterial strains

Four initially selected strains, *Lacticaseibacillus paracasei* BEPC22 (BEPC22), *Lactiplantibacillus plantarum* BELP53 (BELP53), *Lactobacillus helveticus* BELH04 (BELH04), and *Limosilactobacillus fermentum* BELF01 (BELF01), were isolated from Korean faeces. The patents deposited in the Korean Collection for Type Cultures (KCTC) are as follows: *Lacticaseibacillus paracasei* BCC-LP-02 (KCTC 14808BP), *Lactiplantibacillus plantarum* BCC-LPL-53 (KCTC 14809BP), *Lactobacillus helveticus* BCC-LH-04 (KCTC 148010BP), and *Limosilactobacillus fermentum* BCC-LF-01 (KCTC14461BP). The NCBI GenBank accession numbers for these sequences are OL988622, OL988624, OL988623, and OL988625, respectively.

Fatty acid absorption assay

Each strain was activated anaerobically in an MRS medium at 37 °C for 18 h. Subsequently, 1% of the culture was inoculated in MRS medium containing 0.5% (w/v) Brij 58 (Sigma-Aldrich, St Louis, MO, USA) and 0.25 mmol L^{-1} sodium palmitate (Tokyo Chemical Industry Co., Ltd, Tokyo, Kanagawa, Japan) and then incubated at 37 °C for 24 h. The concentrations of fatty acids in the culture media were measured using the EnzyChrom™ free fatty acid assay kit (Bio-Assay Systems, Hayward, CA, USA). The remaining palmitic acid (standard) in the culture medium was quantified to select fatty acid-absorbing bacteria.

Metabolite analyses of the bacterial culture medium

Four strains (BELP53, BEPC22, BELF01, and BELH04) with potential anti-obesity effects were anaerobically cultured in MRS medium at 37 °C for 20 h. The growth of each strain was measured by obtaining the absorbance at 600 nm, and 1 mL of the supernatant was collected at different cell growth phases, including starting, mid-exponential, late-exponential, early stationary, and stationary, for metabolite analyses.

The filtered supernatant (500 μL) was dried and then dissolved in 100% methanol to obtain a 10 000 ppm solution. The derivatisation for gas chromatography time-of-flight mass spectrometry (GC-TOF-MS) was conducted as follows: (1) incubation for 90 min at 30 °C after adding 50 μL of 20 mg mL^{-1} methoxyamine hydrochloride in pyridine and (2) incubation for 30 min at 37 °C after adding 50 μL of *N*-Methyl-*N*-(trimethylsilyl)trifluoroacetamide (Sigma-Aldrich). For instrumental analysis, an Agilent 7890A GC system (Agilent Technologies, Santa Clara, CA, USA) coupled with an Agilent 7693 auto-sampler and a Pegasus® HT TOF-MS (LECO Corp., St Joseph, MI, USA) was utilised. An Rtx-5MS (J&W Scientific, Folsom, CA, USA) column was used. The GC-TOF-MS analysis settings were modified based on previous studies.[18,19] Each sample was analysed in triplicate.

Glucose uptake and pancreatic lipase activity assays

Each strain was co-cultured with Caco-2 cells obtained from the American Type Culture Collection (ATCC, Manassas, VA, USA) for glucose uptake analysis. Caco-2 cells were cultured in a 24-well plate for 15 days until a 3D cell surface layer was formed, with monitoring of the changes in the media every 2 days. LAB (1.0×10^7 CFU^{-1} mL) were co-cultured with Caco-2 cells for 6 h, and then the bacteria and medium were removed. Intracellular glucose concentrations in Caco-2 cells were measured using a Glucose Uptake-Glo Assay Kit (Promega, Madison, WI, USA). All experiments were independently performed in triplicate.

Pancreatic lipase activity was examined following the method described by Han *et al.*[20] Subsequently, 100 μL of the bacterial suspension in TES buffer and 50 μL of pancreatic lipase (10 units) were mixed with 100 μL of fat emulsion, and

then the mixture was incubated at 37 °C for 30 min. The reaction was terminated by incubation in boiling water (100 °C) for at least 2 min. The blank sample was heated immediately after the addition of lipase. The amount of fatty acids in the mixture was measured using the EnzyChrom™ free fatty acid assay kit (Bio-Assay Systems).

Adipocyte differentiation assay

The selected strains were cultured as previously described for 18 h, sterilised at 121 °C, and then freeze dried. Adipocyte differentiation analysis was performed as previously described by Song *et al.*[21] 3T3-L1 pre-adipocytes (ATCC) were cultured in Dulbecco's modified Eagle's medium (DMEM) supplemented with 0.5 mmol L^{-1} 3-isobutyl-1-methylxanthine (Sigma-Aldrich) and 1 mol L^{-1} dexamethasone (Sigma-Aldrich) for 2 days. Then, the medium was replaced with DMEM containing 10% FBS and 1 g mL^{-1} insulin (Sigma-Aldrich) with or without lyophilised powder (1 mg mL^{-1}) of the four LAB. After 4 days of treatment with the differentiation medium, fresh DMEM containing 10% FBS was added, and the medium was replaced every 2 days. The differentiated 3T3-L1 cells were fixed in 10% formaldehyde, and then stained with Oil Red O solution. After treating the cells with isopropanol, the lipid content was measured by obtaining the absorbance at 510 nm.

Animal and experimental design

Specific pathogen-free male C57BL/6J mice (6-weeks old, 20–25 g, n = 30) (Charles River) were allowed *ad libitum* access to food and water. The animal experiments were approved by the Institutional Animal Care and Use Committee (IACUC) of Daegu-Gyeongbuk Medical Innovation Foundation (DGMIF) (approval no. DGMIF-21092702-00). All efforts were made to minimise pain, and the mice were euthanised in accordance with the endpoint criteria of an IACUC-approved protocol. All animal experiments were conducted in accordance with Korea's Animal Protection Act no. 18853 and Laboratory Animal Act no. 18969.

The mice were randomly assigned to one of the following five groups (n = 6 per group): (1) normal diet (ND), (2) high fat diet (HFD), (3) HFD group treated with BEPC22 (HFDPC), (4) HFD group treated with BELP53 (HFDLP), and (5) HFD group treated with the formulation (HFDF). The mice in HFDPC and HFDLP groups were orally administered with 2×10^9 CFU per 200 μL of BEPC22 and BELP53, respectively, daily for 10 weeks. In the HFDF group, mice were orally administered with 2×10^9 CFU per 200 μL of BEPC22 and BELP53 at a ratio of 6 : 4. The mice in the ND group were fed a standard diet (SAFE A40, SAFE Inc., Augy, France) containing 3.2% fat, whereas those in the HFD group were freely provided 60 kcal% fat rodent diet (D12492, Research Diets Inc., New Brunswick, NJ, USA) containing 60% fat, 20% protein, and 20% carbohydrates.

The body weight and food intake of the mice were measured twice a week. The food efficiency ratio was calculated as the total body weight gained from the diet divided by the total diet consumed during the experiments.

After 10 weeks of treatment, the liver and white adipose tissues (epididymal, mesenteric, perirenal, and subcutaneous) were dissected and weighed, and then frozen in liquid nitrogen for qRT-PCR. The epididymal adipose tissue was fixed in 10% neutral buffered formalin (BBC Biochemical, Mount Vernon, WA, USA) for histological analysis. Blood samples were collected from the abdominal aortas of the mice under isoflurane (Hana Pharm, Co., Ltd, Seoul, Korea) anaesthesia and then centrifuged for 3 min at 8000*g* for plasma separation. Faecal samples were obtained from each of the 30 mice directly into sterile 1.5 mL Eppendorf tubes and stored at−80 °C until use.

Plasma biochemical analysis

Plasma levels of GIP, GLP-1, glucagon, insulin, leptin, PAI-1, and resistin were measured using a Bio-plex Pro Mouse Diabetes 8-plex Assay Kit (Bio-Rad Laboratories, Hercules, CA, USA). Adiponectin levels were measured using an adiponectin ELISA kit (Thermo Fisher Scientific, Waltham, MA, USA) in accordance with the manufacturer's instructions.

Histological analysis

For histological analysis, epididymal adipose tissue was prepared using a tissue processor (Thermo Fisher Scientific). Sections (4 μm) were obtained from paraffin-embedded blocks and then stained with haematoxylin and eosin using an autostainer (Dako Coverstainer, Agilent, Santa Clara, CA, USA). Adipocyte size was measured using an IX83 microscope (Olympus Corporation, Tokyo, Kanagawa, Japan).

Transcriptional analysis

Total RNA was extracted from the liver and epididymal adipose tissues by using a RNeasy Mini Kit and RNeasy Lipid Tissue Mini Kit (Qiagen, Hilden, Nordrhein-Westfalen, Germany), respectively, in accordance with the manufacturer's instructions. The extracted RNA was reverse-transcribed using a SuperScript IV First-Strand Synthesis Kit (Thermo Fisher Scientific). Quantitative PCR (qPCR) was performed using an Exicycler 384 qPCR system (Bioneer, Daejeon, Korea) with the AccuPower 2X GreenStar qPCR Master Mix (Bioneer). The relative expression levels of the target genes (*Ppar-α*, *Ppar-γ*, *Cpt1a*, and *Ucp2*) were calculated using the $2^{-\Delta\Delta CT}$ method. *Gapdh* was used as the internal reference gene.

Metabolite extraction

Metabolites were extracted from the plasma as follows. Mouse plasma (100 μL) was added with methanol (500 μL) containing 10 ppm of 2-chlorophenylalanine as an internal standard. The mixture was homogenised using a Retsch MM400 Mixer Mill (Retsch GmbH & Co., Haan, Nordrhein-Westfalen, Germany) at 30 s^{-1} for 10 min and then sonicated for 10 min (Hettich Zentrifugen Universal 320, Tuttlingen, Baden-württemberg, Germany). The samples were allowed to settle at −20 °C for 1 h. Subsequently, the mixtures were centrifuged at 27 000*g* for 10 min at 4 °C.

Metabolites were extracted from the faeces as follows. Faecal samples (100 mg) were added with 1 mL of methanol (containing the same amount of the internal standard). Subsequent procedures were the same as those used in plasma extraction but without resting in a freezer.

The supernatants were filtered into new Eppendorf tubes using Millex GP 0.22 μm filters (Merck Millipore, Billerica, MA, USA) and dried utilising a speed vacuum concentrator (Biotron, Seoul, Korea). The dried samples were re-dissolved in 100% methanol to obtain a final concentration of 5000 ppm.

Metabolome analysis

For GC-TOF-MS analysis, 100 μL of the re-dissolved samples was dried again using a speed vacuum concentrator. The dried samples were derivatised as described earlier. The analytical parameters were adapted from a previous study.[19]

Ultra-high-performance liquid chromatography-linear trap quadrupole-orbitrap-tandem mass spectrometry (UHPLC-LTQ-Orbitrap-ESI-MS/MS) was performed using a Vanish binary pump H system (Thermo Fisher Scientific) coupled with an autosampler and column compartments. A Phenomenex KINETEX® C18 column (100 mm × 2.1 mm, 1.7 μm particle size; Torrance, CA, USA) was used to separate the sample analytes. The injection volume was 5 μL. The column temperature was maintained at 40 °C, and the flow rate was 0.3 mL min^{-1}. The MS data were collected at 100–1500 *m*/*z* in negative and positive ion modes by using an Orbitrap Velos Pro™ system combined with an ion-trap mass spectrometer (Thermo Fisher Scientific) coupled with an HESI-II probe. The analytical parameters were adopted from a previous study.[18]

Raw data obtained from GC-TOF-MS and UHPLC-LTQ-Orbitrap-ESI-MS/MS were converted to NetCDF (*.cdf). Subsequently, the NetCDF files were processed using MetAlign software (**https://www.metalign.nl**, Wageningen, Netherlands) for data alignment in accordance with peak mass (*m*/*z*) and retention time (min).[28] Metabolites were tentatively identified by comparison with various analysis data, such as molecular weight, formula, retention time, mass fragment patterns, and mass spectra of the standard compounds; previous publications; an in-house library; and commercial databases, such as the National Institutes of Standards and Technology Library (version 2.3, FairCom, Gaithersburg, MD, USA) and the Human Metabolome Database (**https://www.hmdb.ca/** (accessed on Sep 2022)).

Extraction of genomic DNA from mouse faecal samples

Total genomic DNA was extracted from 200 mg of faecal samples using a Maxwell® RSC PureFood GMO and Authentication Kit (Promega) following the manufacturer's instructions. The concentration and quantity of DNA were determined using a UV-vis spectrophotometer (NanoDrop 2000c, Wilmington, DE, USA) and a QuantiFluor® ONE dsDNA System (Promega), respectively.

Gut microbiota analysis using next-generation sequencing

The gut microbiota composition of the mice was analysed through 16S rRNA amplicon sequencing using an Illumina MiSeq platform (Illumina, San Diego, CA, USA) in accordance with the manufacturer's instructions. The V3–V4 region of the bacterial 16S rRNA gene was amplified using the primer set F319 and R806.

The gut microbiota data were analysed using the QIIME 2 2022.02 pipeline.[22] Paired-end sequence data were demultiplexed using MiSeq Reporter and joined using the 12-vsearch plugin. Merged sequences were filtered using the q2-quality-filter plugin and then denoised with Deblur (*via* q2-deblur).[23] All amplicon sequence variants (ASVs) were aligned with mafft (*via* q2-alignment).[24] Alpha–diversity metrices (Shannon and Simpson diversity), beta-diversity metrics (Bray–Curtis dissimilarity), and principal coordinate analysis (PCoA) were estimated using q2-diversity after the samples were rarefied (subsampled without replacement).[25–27] Taxonomy was assigned to ASVs using the q2-feature–classifier classify–sklearn naïve Bayes taxonomy classifier against the SILVA database v138.[28,29] Significant differences in the bacterial structure and taxonomy were determined using permutational multivariate analysis of variance and linear discriminant analysis (LDA) effect size (LEfSe) analysis (LDA score > 3.0), respectively.[30,31] The correlation between variables was assessed using the 'cor' function of R, and the Spearman correlation coefficient was calculated using the 'psych' (v2.2.9) package to assess the correlation strength. The Benjamini–Hochberg correction was conducted to account for multiple testing. Heatmaps were generated using the 'pheatmap' (1.0.12) package to visualise the correlation patterns between variables.

Statistical analysis

Statistical analysis of *in vivo* data was performed using Prism 9 software (GraphPad Software Inc., San Diego, CA, USA). For comparisons of more than two groups, a one-way or two-way ANOVA was performed, followed by a *post hoc* test with Dunnett's correction for pairwise group differences. All data are expressed as the mean ± SD (standard deviation) or standard error of the mean (SEM), and $p < 0.05$ was considered statistically significant.

Multivariate statistical analysis of the metabolome data was conducted using SIMCA-P + software (version 15.0.2, Umetrics, Umea, Sweden). Principal component analysis (PCA) and partial least squares discriminant analysis (PLS-DA) were conducted to compare the metabolites among the samples. The discriminant metabolites were selected based on the variable importance in the projection (VIP) value > 0.7 and *p*-value < 0.05.

Results

Fatty acid absorption by *Lactobacillus* strains

The fatty acid absorption capacities of more than 300 strains of *Lactobacillus*, *Lactiplantibacillus,* *Lacticaseibacillus*,

Limosilactobacillus, *Ligilactobacillus*, *Lactococcus*, and *Bifidobacterium* species were evaluated by culturing them in MRS broth containing 0.25 mmol L^{-1} sodium palmitate for 24 h and measuring the fatty acid concentration in the culture broth. Interestingly, *Lactobacillus* spp. showed a higher free fatty acid (FFA) absorption capacity than *Lactococcus* and *Bifidobacterium* spp. (data not shown). Strains of *Lactiplantibacillus plantarum* (*LPL*), *Lacticaseibacillus paracasei* (*LP*), *Limosilactobacillus fermentum* (*LF*), and *Lactobacillus helveticus* (*LH*) showed notable decreases in total fatty acids in the medium (Fig. 1A). Specifically, *LP* and *LPL* strains absorbed 83.9%–86.6% ($p < 0.01$) of fatty acids in the medium. Thus, the strains of *LPL*, *LP*, *LF*, and *LH* with the highest FFA absorption capacity (BELP53, BEPC33, BELF01, and BELH04, respectively) were selected for further analyses.

Pancreatic lipase inhibition by selected strains

Considering the key roles of pancreatic lipase in intestinal lipid metabolism and absorption, we investigated the inhibitory effects of the four selected strains on pancreatic lipase activity using fat emulsions.[32] BEPC22, BELP53, and BELH04 inhibited pancreatic lipase activity by 25.8%, 45.0%, and 34.4%, respectively, compared with the negative control (strain-untreated), whereas BELF01 exerted no inhibitory effect on pancreatic lipase activity (Fig. 1B).

Selection of the best pair of two strains

To identify the optimal pairs among the four strains, we compared their metabolic characteristics, including nutritional source utilisation and byproduct generation patterns, during cell growth. Metabolite analyses were conducted at the start, mid-exponential, late exponential, early stationary, and stationary growth phases of each strain (Fig. 2A). Primary metabolites essential for cell survival in the culture medium of the four selected anti-obesity candidates (BELH04, BEPC22, BELP53, and BELF01) were analysed using GC-TOF-MS. Significantly different metabolites were selected based on the VIP value (>0.7) using PLS-DA and *p*-value (<0.05) to investigate the metabolite changes of the four strains. We profiled 74 distinct metabolites, containing amino acids, organic acids, and carbohydrates, and analysed the metabolite consumption and production patterns of the strains (data not shown). Metabolites produced by all strains and/or fluctuating over the cell cultivation period were not of interest because they might not affect other strains in the microorganism formulation. Consequently, five metabolites (aconitic acid, malic acid, gluconic acid, orotic acid, and glyceric acid) were listed as potentially important for microorganism pairing based on the consumption and production patterns of each strain (Fig. 2B). Six pairs were formed from the four strains, but three of these pairs were excluded (BELH04–BELF01, BEPC22–BELP01, and BELP53–BELF01) because their same consumption patterns as the five abovementioned metabolites may cause competition between members and amensalism. Thus, three noncompeting pairs (BELH04–BEPC22, BELH04–BELP53 and BEPC22–BELP53) were used in the subsequent experiments. In the BELH04–BEPC22 pair, orotic acid and glyceric acid produced by BEPC22 can feed on BELH04, potentially forming commensalism. Intriguingly, between the BELH04 and BELP53 pair, the aconitic acid produced from BELH04 can be used by

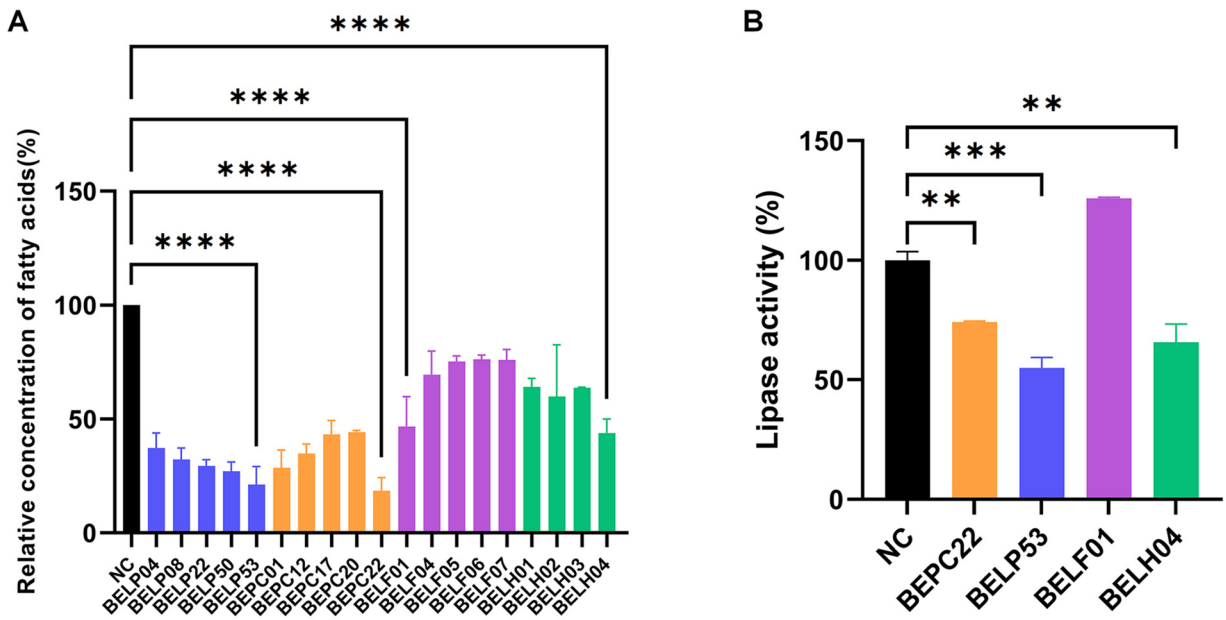

Fig. 1 Screening of the *Lactobacillus* strains inhibiting fat absorption. (A) Fatty acid absorption by *Lactobacillus* during cultivation. (B) Pancreatic lipase activity of the strains. Values represent the mean ± SD of three independent experiments. Significance is indicated by *$p < 0.05$, **$p < 0.01$, and ***$p < 0.001$ as compared with the untreated group. *LP, Lactiplantibacillus plantarum*; *PC, Lacticaseibacillus paracasei*; *LF, Limosilactobacillus fermentum*; *LH, Lactobacillus helveticus*.

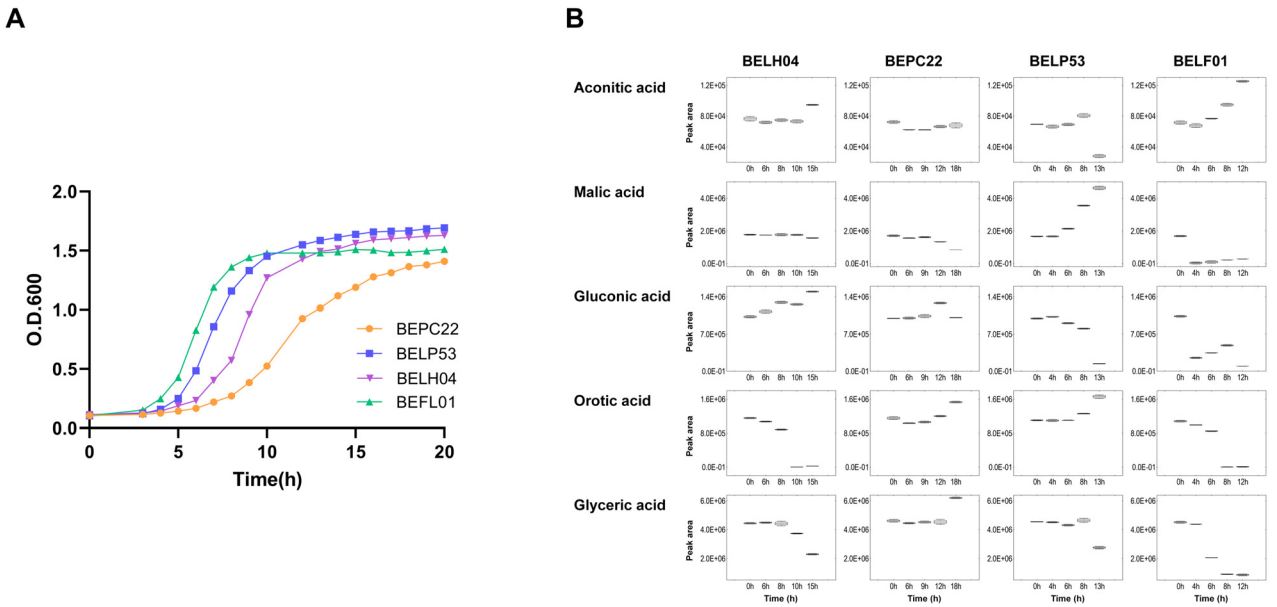

Fig. 2 Metabolic characteristics of the selected strains during cultivation. (A) Bacterial growth curves of the four candidates with potential anti-obesity effects. (B) Consumption and production patterns of potentially important metabolites for constructing microbial relationships during cell growth of the four candidates.

BELP53, while BELH04 can take up orotic acid which was excreted by BELP53. Similarly, in the BEPC22–BELP53 pair, glyceric acid produced by BEPC22 can be consumed by BELP53, whereas malic acid produced by BELP53 can be utilised by BEPC22. To select the best pair of the two pairs, we considered the distance of each metabolite from the central metabolism based on the hypothesis that the metabolite close to the central metabolism may be utilized more easily and more demanding by the microorganism. According to the hypothesis, orotic acid, produced in the pyrimidine metabolism, is distant from the central metabolism as compared to the malic acid and glyceric acid. Thus, we assumed that BEPC22 and BELP53 can form the best mutualism by cross-feeding glyceric acid and malic acid.

Glucose uptake inhibition by the selected strains

Fatty acids converted from excess sugar promote triglyceride synthesis and contribute to adipocyte accumulation.[33] In the present study, the inhibitory effects of BEPC22, BELP53, BELF01 and BELH04 on glucose uptake were investigated in human colon epithelial Caco-2 cells. Treatment of Caco-2 cells with BELP53 and BELF01 decreased glucose uptake by 37.9% and 43.1%, respectively (Fig. 3A).

Adipocyte differentiation inhibition by selected strains

Adipocyte differentiation is essential in obesity development. Therefore, inhibition of this process could be an anti-obesity mechanism of various LAB.[4,34,35] In the present study, the inhibitory effects of BEPC22, BELP53, BELF01 and BELH04 on adipocyte differentiation were investigated in 3T3-L1 pre-adipocytes. Results showed that BEPC22, BELP53, BELF01 and BELH04 significantly decreased lipid contents in pre-adipocytes by 78.7%, 64.9%, 17.7% and 72.4%, respectively ($p < 0.05$; Fig. 3B). BELP22 showed the strongest inhibition of adipocyte differentiation. Therefore, we selected BEPC22 and BELP53 as the best probiotic pair for further analyses for their functionality properties.

Formulation synergistic effect with BEPC22 and BELP53

In the present study, the inhibitory effects of BEPC22 and BELP53 on adipocyte differentiation were evaluated. Results showed that BEPC22 and BELP53 significantly decreased lipid contents in 3T3-L1 pre-adipocytes ($p < 0.01$; Fig. 3D). These two strains were not cytotoxic to 3T3-L1 cells (data not shown). To determine the optimum formulation (F) ratio of the probiotics with anti-obesity effects, we treated 3T3-L1 pre-adipocytes with a combination of BEPC22 and BELP53 at different ratios of 8 : 2 (F1), 6 : 4 (F2), 4 : 6 (F3), and 2 : 8 (F4). Each formulation-treated group exhibited a different degree of adipocyte differentiation (Fig. 3B and C). Interestingly, the 3T3-L1 cells treated with F2, F3, and F4 exhibited lower differentiation than those treated with the individual strains, suggesting a potential synergistic action between BEPC22 and BELP53. Among the formulations, F2 (6 : 4) demonstrated the strongest inhibitory effect (91.3%) on adipogenesis.

Inhibition of body weight gain and fat accumulation by probiotic administration in HFD-induced obese mice

We investigated the anti-obesity effects of the probiotics as individual strains or in combination on HFD-fed mice. As shown in Fig. 4A, the body weight gain of the mice in the HFD group was significantly higher than that of the mice in the ND

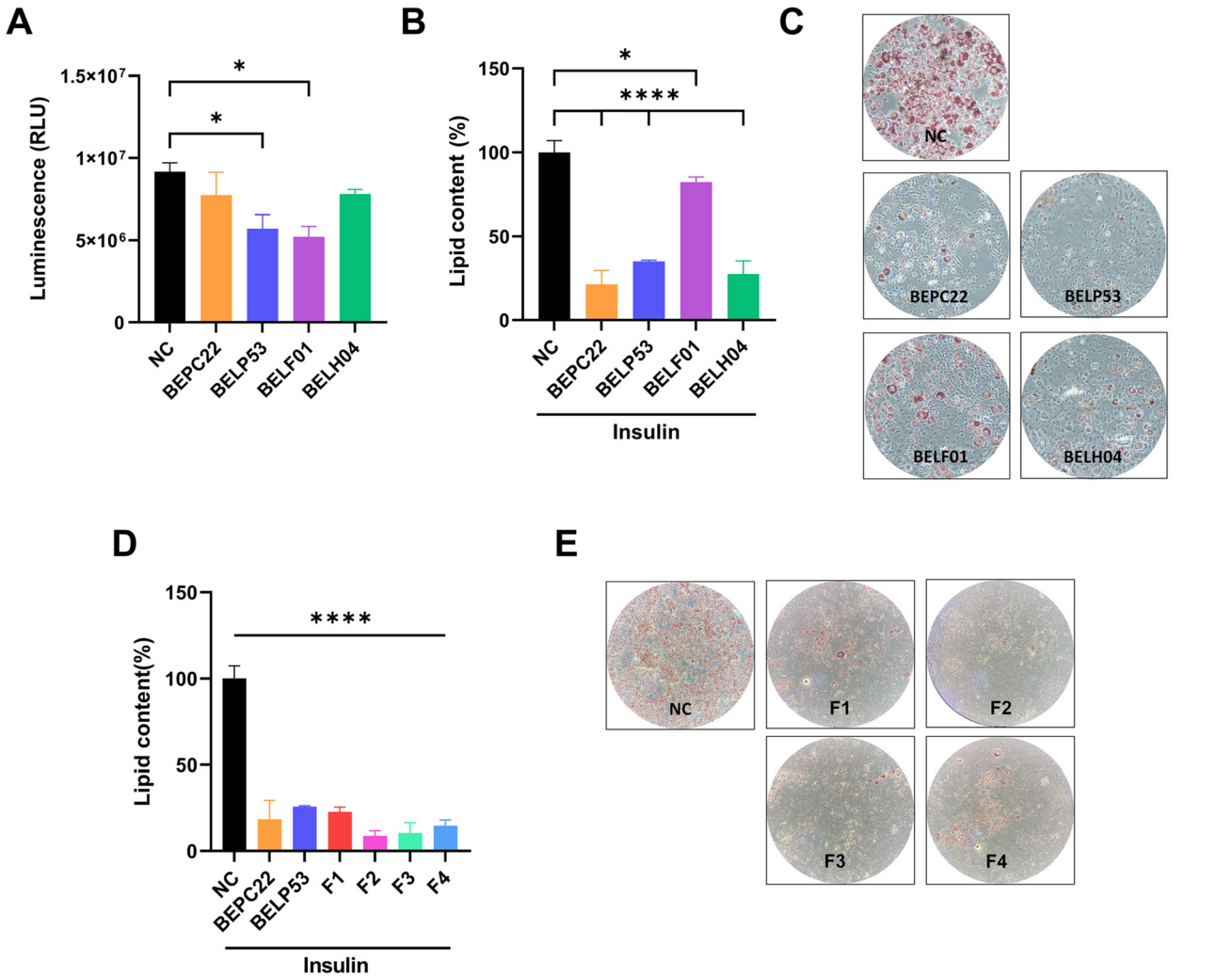

Fig. 3 Glucose absorption and adipocyte production of the selected strains. (A) Glucose uptake inhibition of strains in Caco-2 cells. (B) Adipocyte differentiation inhibitory activity by the strains. (C) Images of the cell culture plate of 3T3-L1 cells after staining lipid droplets with oil red O. (D) Adipocyte differentiation inhibitory activity by the formulation of BEPC22 and BELP53 in a synergistic way. (E) Images of the cell culture plate of 3T3-L1 cells after staining lipid droplets with oil red O. Quantitative analysis of lipid accumulation was performed by measuring absorbance on a microplate reader. Values represent the mean ± SD of three independent experiments. Significance is indicated by $*p < 0.05$ and $**p < 0.01$ as compared with the untreated group.

group at 10 weeks after treatment ($p < 0.0001$). The mice in the HFDPC and HFDLP groups showed relatively lower body weights than those in the HFD group, but the differences were not statistically significant. At 38 days after treatment, the body weights of the mice in the HFDF group significantly decreased compared with those in the HFDPC and HFDLP groups. After 10 weeks, the body weight gain of the mice in the HFDF group was approximately 36.4% lower than that of the mice in the HFD group ($p < 0.0001$). Meanwhile, the food intake of the mice in the HFDPC and HFDLP groups was similar to that of the mice in the HFD group, whereas the mice in the HFDF group showed 1.8-fold higher food intake than those in the HFD group at 10 weeks. Surprisingly, the food efficiency ratio of the mice in the HFDF group was 50% lower than that of the mice in the HFD group, and it was similar to the that of the mice in the ND group ($p < 0.0001$, Fig. 4B). Taken together, formulation administration to the HFD-fed mice helped them gain much less weight even though their food intake increased by almost twofold.

Compared with ND, HFD increased the weights of all white adipose tissues, including the subcutaneous, epididymal, mesenteric, and perirenal ones (Fig. 4C). The weights of all white adipose tissues showed negligible changes in the HFDLP group, whereas only the weight of the subcutaneous white adipose tissue significantly decreased in the HFDPC group. In contrast, the mice in the HFDF group had 48%, 66%, 42%, and 60% lower weights of the subcutaneous, epididymal, mesenteric, and perirenal adipose tissues, respectively, than the mice in the HFD group ($p < 0.0001$ for subcutaneous,

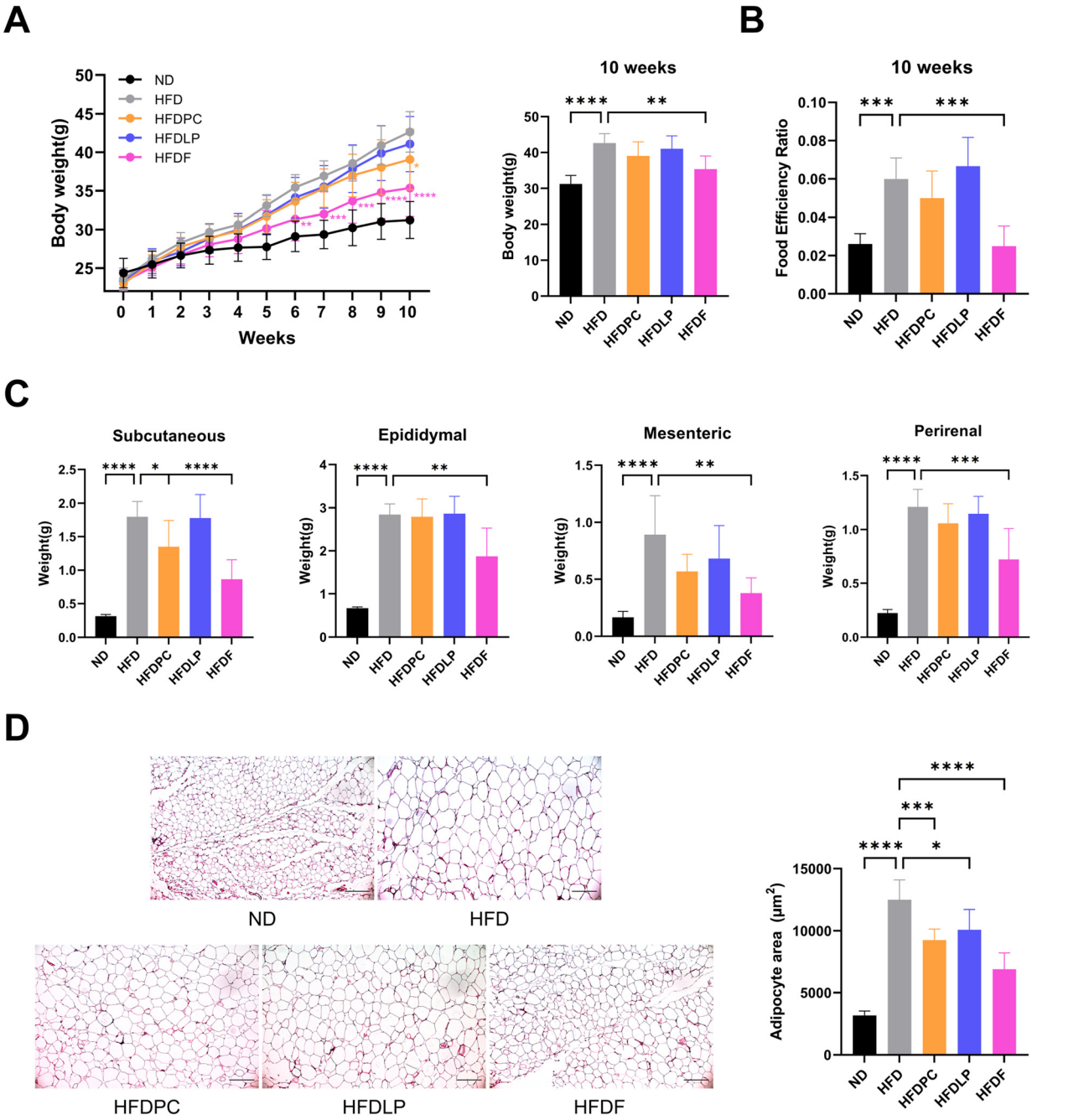

Fig. 4 Effect of the probiotic formulation on high-fat diet-fed obese mice. (A) Body weight gain in mice, (B) food efficiency ratio at day 70, (C) weight of the four types of the white adipose tissue, and (D) representative haematoxylin & eosin staining images of the epididymal adipose tissue and adipocyte mean area. Values represent the mean ± SD (n = 6 per group). Significance is indicated by *p < 0.05, **p < 0.01, ***p < 0.001, and ****p < 0.0001 as compared with the ND group. Scale bars: 200 μm. HFD, high fat diet; HFDPC, HFD with *Lacticaseibacillus paracasei* BEPC22; HFDLP, HFD with *Lactiplantibacillus plantarum* BELP53; HFDF, HFD with the combination of two strains.

p < 0.01 for mesenteric, epididymal, and perirenal). Additionally, haematoxylin and eosin (H&E) staining revealed that the average adipocyte size was dramatically larger in the HFD group than in the ND group, whereas the adipocyte sizes in the HFDPC, HFDLP, and HFDF groups were approximately 25%, 20%, and 40% smaller, respectively, than those in the HFD group (Fig. 4D).

Reduction in the plasma levels of obesity-related hormones by probiotics

To understand the mechanisms underlying the anti-obesity effects of the formulation, we first measured the plasma levels of obesity-related hormones, such as adiponectin, ghrelin, GIP, insulin, leptin, PAI-1, resistin, and glucagon. The plasma

levels of these hormones, except for PAI-1 and glucagon, showed opposite patterns in the HFD and ND groups (Fig. 5 and ESI Fig. 1†). Treatment with the probiotics significantly altered the plasma levels of ghrelin and leptin but not those of adiponectin, insulin, PAI-1, resistin, GIP, and glucagon. The plasma level of ghrelin was approximately 1.53-fold higher in the HFDF group than in the HFD group ($p < 0.05$, Fig. 5A). The plasma level of leptin was approximately 50% lower in the HFDF group than in the HFD group ($p < 0.05$, Fig. 5B).

Effect of probiotics on the mRNA expression of obesity-related genes

We analysed the expression patterns of obesity-related genes in the liver and adipose tissue to understand the mechanisms by which probiotic administration reduces body weight gain. In the liver, the mRNA expression of *Ppar-γ* in the HFDF group was significantly lower than that in the HFD group ($p < 0.05$), whereas the mRNA expression of *Ppar-γ* in the HFD group was significantly higher than that in the ND group (Fig. 6A, $p < 0.01$). The mRNA expression of *Ucp2* in the HFDPC, HFDLP, and HFDF groups was significantly lower than that in the HFD group ($p < 0.05$ for HFDPC and HFDLP, $p < 0.001$ for HFDF, Fig. 6B). However, the relative expression levels of *Ppar-α* and *Cpt1a* showed no significant changes in the groups, except for the ND group (ESI Fig. 2A and B†).

In the epididymal adipose tissue, the mRNA expression of *Ppar-α* in the HFDF group was approximately 2.5-fold higher than that in the HFD group ($p < 0.0001$, Fig. 6C), whereas the mRNA expression of *Ucp2* in the HFDF group was significantly lower than that in the HFD group ($p < 0.001$, Fig. 6D). In addition, the mRNA expression of *Ppar-γ* in the HFDF group was approximately 80% higher than that in the HFD group ($p < 0.001$, ESI Fig. 2C†), whereas the mRNA expression of *Cpt1a* in the HFD, HFDPC, HFDLP, and HFDF groups was higher than that in the ND group (ESI Fig. 2D†).

Changes of the metabolome by probiotics

To identify the metabolites relevant to reduced weight gain, we performed non-targeted metabolomic analysis using mouse faeces and plasma. Multivariate statistical analysis revealed different patterns depending on the specimens and analytical instruments used (Fig. 7). PLS-DA of the faecal metabolomic data obtained using GC-TOF-MS showed a clear distinction between the HFDF and HFD groups (Fig. 7A). Interestingly, PLS-DA of the faecal metabolomic data obtained using UHPLC-LTQ-Orbitrap-MS/MS showed dissimilar patterns. The HFDF group clustered with the HFDLP group, and they were separate from the HFD and HFDPC groups (Fig. 7A). A total of 39 distinct metabolites were identified in the faeces, of which 20 and 19 were identified using GC-TOF-MS and UHPLC-LTQ-Orbitrap-MS/MS, respectively (ESI Tables 1 and 2†). The identified metabolites included 2 organic acids, 9 amino acids, 16 lipids (4 fatty acids and their derivatives, 10 glycerophospholipids, 1 sphingolipid, and 1 bile acid), 1 carbohydrate, 2 nucleotides, 2 benzenoids, 1 flavonoid, and 3 bacteriocins. Most amino acids, carbohydrates, benzenoids, bacteriocins, and some lipids were more abundant in the HFD group than in the other probiotic-treated groups. The HFDPC group showed significantly reduced levels of organic acids, amino acids, carbohydrates, nucleotides, benzenoids, bacteriocins, and some lipids in the faeces (Fig. 7B). In contrast, the HFDLP group showed lower reduction in the amounts of carbohydrates and some amino acids and alteration in lipid composition than the HFDPC group. The lipid composition in the HFDF group was similar to that in the HFDLP group. Notably, the HFDF group showed increased levels of guanosine and decreased levels of bacteriocins.

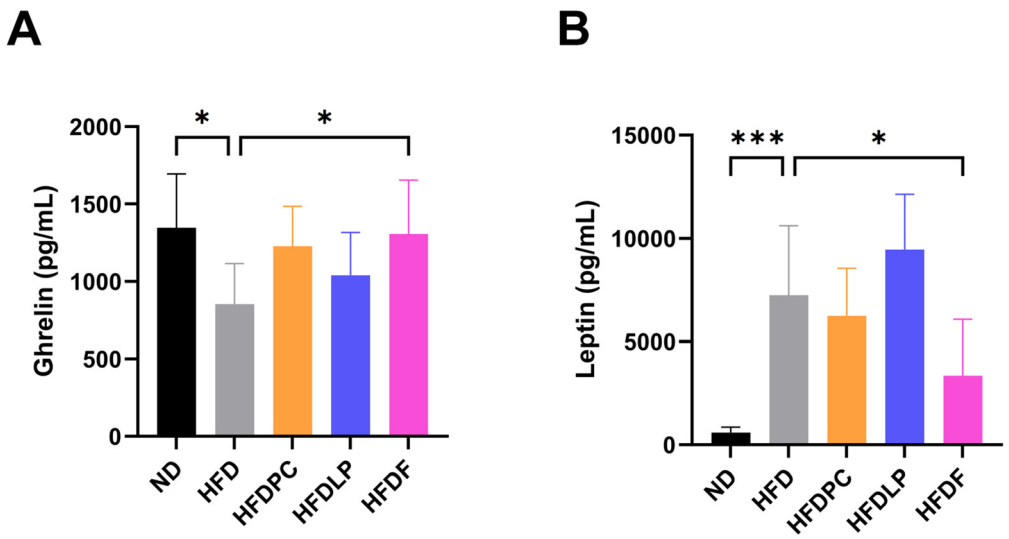

Fig. 5 Obesity-related hormone level in the plasma of probiotic-administered mice. (A and B) Graphs showing the results of the quantitative analysis of the statistically significant levels of the hormones ghrelin and leptin. Values represent the mean ± SD ($n = 6$ per group). Significance is indicated by *$p < 0.05$, **$p < 0.01$, and ***$p < 0.001$ as compared with the ND group. HFD, high fat diet; HFDPC, HFD with *Lacticaseibacillus paracasei* BEPC22; HFDLP, HFD with *Lactiplantibacillus plantarum* BELP53; HFDF, HFD with the combination of two strains.

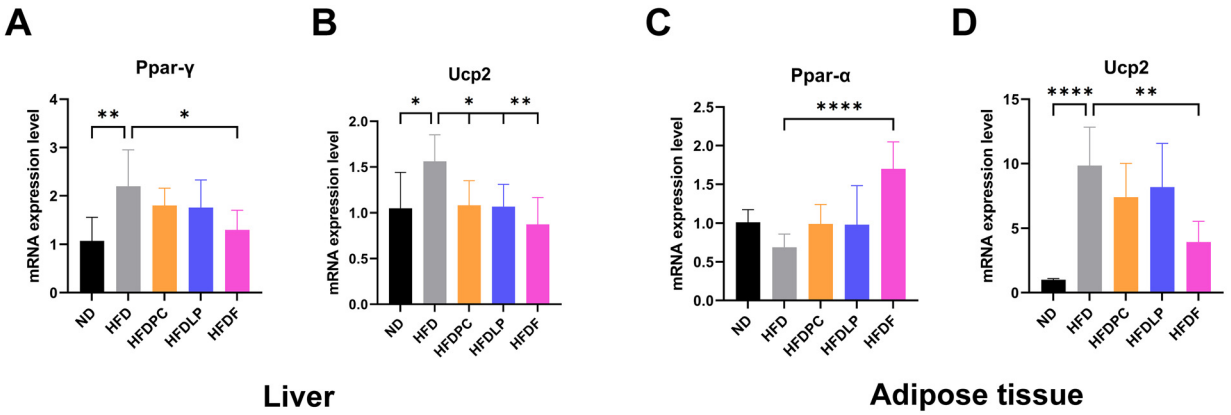

Fig. 6 mRNA expression of obesity-related genes in the liver and white adipose tissue. qPCR analysis of *Ppar-γ* and *Ucp2* expression in the (A and B) liver and (C and D) epididymal adipose tissue. Values represent the mean ± SD (n = 6 per group). Significance is indicated by *p < 0.05, **p < 0.01, ***p < 0.001, and ****p < 0.0001 as compared with the high-fat diet group. HFD, high fat diet; HFDPC, HFD with *Lacticaseibacillus paracasei* BEPC22; HFDLP, HFD with *Lactiplantibacillus plantarum* BELP53; HFDF, HFD with the combination of two strains; *Ppar-α* or *γ*, peroxisome proliferator-activated receptor alpha or gamma; *Ucp2*, uncoupling protein2; *Cpt1a*, carnitine palmitoyltransferase1a.

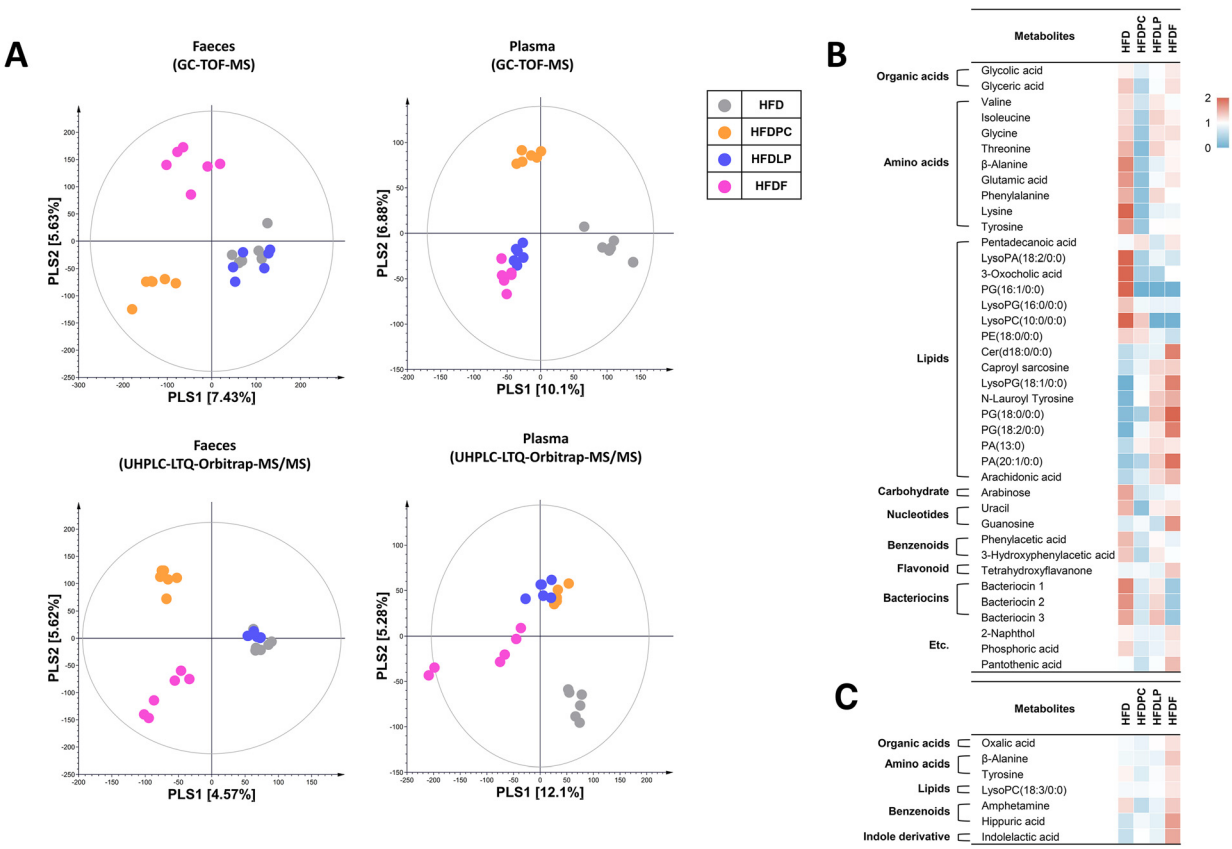

Fig. 7 Metabolome alteration by probiotic administration. (A) Sparse partial least-squares discriminant analysis (PLS-DA) score plots for the metabolome of faeces and plasma of the four (HFD, high fat diet; HFDPC, HFD with *Lacticaseibacillus paracasei* BEPC22; HFDLP, HFD with *Lactiplantibacillus plantarum* BELP53; HFDF, HFD with the combination of two strains) groups based on GC-TOF-MS and UHPLC-LTQ-Orbitrap-MS/MS data sets. Heatmap analysis of the (B) faeces and (C) plasma based on the GC-TOF-MS and UHPLC-LTQ-Orbitrap-MS/MS data. The heatmap represents the relative abundance of significantly discriminant metabolites (VIP > 0.7, p < 0.05) based on the PLS-DA model.

The PLS-DA score plots of the plasma based on GC-TOF-MS and UHPLC-LTQ-Orbitrap-MS/MS analyses were dissimilar (Fig. 7A). Seven metabolites, including 1 organic acid, 2 amino acids, 1 lipid, 2 benzenoids, and 1 indole derivative, were identified in the plasma (ESI Tables 3 and 4†). Most of the identified metabolites were abundant in the HFDF group (Fig. 7C).

To evaluate the metabolites relevant to weight gain reduction, we conducted correlation analyses using discriminant metabolites in the faeces and plasma based on the mouse phenotype data. In the faeces, Cer(d18 : 0/0 : 0), guanosine, and tetrahydroxyflavone levels were negatively correlated with epididymal and perirenal fat weights (ESI Fig. 3†). Three metabolites, tentatively identified as bacteriocins, were negatively correlated with ghrelin levels. In the plasma, lysoPC (18 : 3/0 : 0), hippuric acid, and indolelactic acid were negatively correlated with fat weight and positively correlated with *Ppar-α* expression (ESI Fig. 4†).

Microbiome changes by probiotics

To investigate the effect of probiotics on the gut microbiota, we conducted a 16S metagenomic analysis of faecal samples. No difference in the Shannon index was found (ESI Fig. 5A†), but PCoA analysis showed a marked difference ($p < 0.001$) at 10 weeks between the HFD and probiotic-treated groups (ESI Fig. 5B†). At the phylum level, fewer Firmicutes species and more Bacteroidota species were observed in the HFDPC, HFDLP, and HFDF groups (Fig. 8A). Thus, the F/B ratio in the probiotic-treated groups was lower than that in the HFD group ($p < 0.05$, only in the HFDPC group, Fig. 8B). At the genus level, the abundance of *Colidextribacter*, *Tuzzerella*, *Alistipes*, *Muribaculaceae*, and *Akkermansia* significantly differed between the probiotic-administered groups. In particular, the abundance of *Colidextribacter* and *Tuzzerella* significantly decreased, whereas that of *Alistipes* significantly increased in the HFDPC and HFDF groups. The abundance of *Muribaculaceae* significantly increased only in the HFDPC group, whereas the abundance of *Akkermansia* significantly increased in the HFDF group compared with the HFDPC and HFDLP groups. In addition, LEfSe analysis showed that the abundance of *Christensenellaceae*, *Paludicola*, *Ruminococcus*, *Butyricicoccus*, *Oscillospiraceae_UCG-005*, *Butyricicoccaceae_UCG-009*, *Oscillospirales_UCG-010*, *Muribaculaceae*, and *Alistipes* significantly increased in the HFDPC group (Fig. 8D); *Atopobiaceae*, *Ruminococcus*, *Coriobacteriaceae*, *Oscillospirales_UCG-010*, *Faecalibacterium*, and *Alistipes* in the HFDLP group; and RF39, *Ruminococcus*, *Butyricicoccaceae_UCG-009*, *Oscillospirales_UCG-010*, *Faecalibacterium*, *Akkermansia*, and *Alistipes* in the HFDF group (Fig. 8D).

Discussion

To develop an anti-obesity probiotic, we selected BEPC22 and BELP53 with synergistic inhibitory effects on fatty acid absorption, glucose uptake and metabolite producing/utilizing potential. Among the metabolites consumed/produced in the medium of the BEPC22–BELP53 pair, glyceric acid produced by BEPC22 can be consumed by BELP53, whereas malic acid produced by BELP53 can be utilised by BEPC22. Thus, we assumed that BEPC22 and BELP53 can form mutualism by cross-feeding glyceric acid and malic acid. Subsequently, an optimal ratio of 6 : 4 with BEPC22 and BELP53 was determined through *in vitro* anti-adipogenic assays.

The effects of the single probiotic strains or formulation on HFD-induced obese mice were assessed. The mice in the HFDF group had the lowest body weight gain possibly because of the decreased weights of the subcutaneous and abdominal adipose tissues in this group, implying the combined treatment of the two strains exhibited a synergistic effect in ameliorating obesity when we compared with the single strain administered results (HFDPC and HFDLP). Within the gut, the administered probiotics affected the gut microbiome to restructure by engaging cross-feeding, which eventually caused reduction of body weight gain.[36]

Among obesity-related biomarkers, leptin is a key anti-obesity hormone that has the greatest impact on body fat weight and regulates appetite. This hormone is produced by adipocytes and secreted into the blood, and its production level correlates with adipocyte size.[37,38] Previous studies have shown that the plasma levels of leptin decrease during weight loss.[38–40] In the present study, the plasma level of leptin in the HFDF group was almost 50% lower than that in the HFD group, indicating that the decrease in body weight gain might be caused by the reduced adipose tissue weight resulting from the smaller adipocyte size. This result indicated that the probiotic treatment was responsible for the decrease in plasma leptin levels.

Leptin in the blood increases the expression of *Ucp2*, the gene which increases the thermogenic capacity of brown adipose tissue and helps reduce body fat.[41,42] In the present study, the leptin level and *Ucp2* expression decreased in the liver and epididymal adipose tissue in the HFDF group. This result suggested that the probiotic treatment decreased the leptin levels, which contributed to the decreased *Ucp2* expression in the liver and epididymal adipose tissue. Promoting fatty acid oxidation and inhibiting fatty acid synthesis, which are mainly mediated by PPAR family members, are necessary to reduce fat weight.[43] In the adipose tissue, *Ppar-α* plays an important role in reducing fat mass and body weight by promoting the oxidation of fatty acids, inhibiting the secretion of triglycerides, and increasing energy expenditure through the regulation of downstream genes, such as *Acox* and *Cpt1*.[44–46] In the present study, we observed a relatively higher *Ppar-α* expression in the epididymal adipose tissue and, consequently, a lower fat weight in the HFDF group than in the HFD group. This result might be due to fatty acid oxidation and increased energy consumption. However, no significant difference in *Cpt1a* expression was found between the probiotic-treated groups and the HFD group, whereas *Cpt1a* expression showed significant differences between the HFD and ND groups. The decrease in body weight and fat weight in the formulation-treated group might have been caused by the relatively higher fatty acid oxidation in the adipose tissue than the reduction in fatty acid synthesis.

The liver takes up, synthesises, stores, and secretes fatty acids and triglycerides. Fatty acid synthesis is mainly contributed by *Ppar-γ*.[47] In the present study, the mRNA expression of

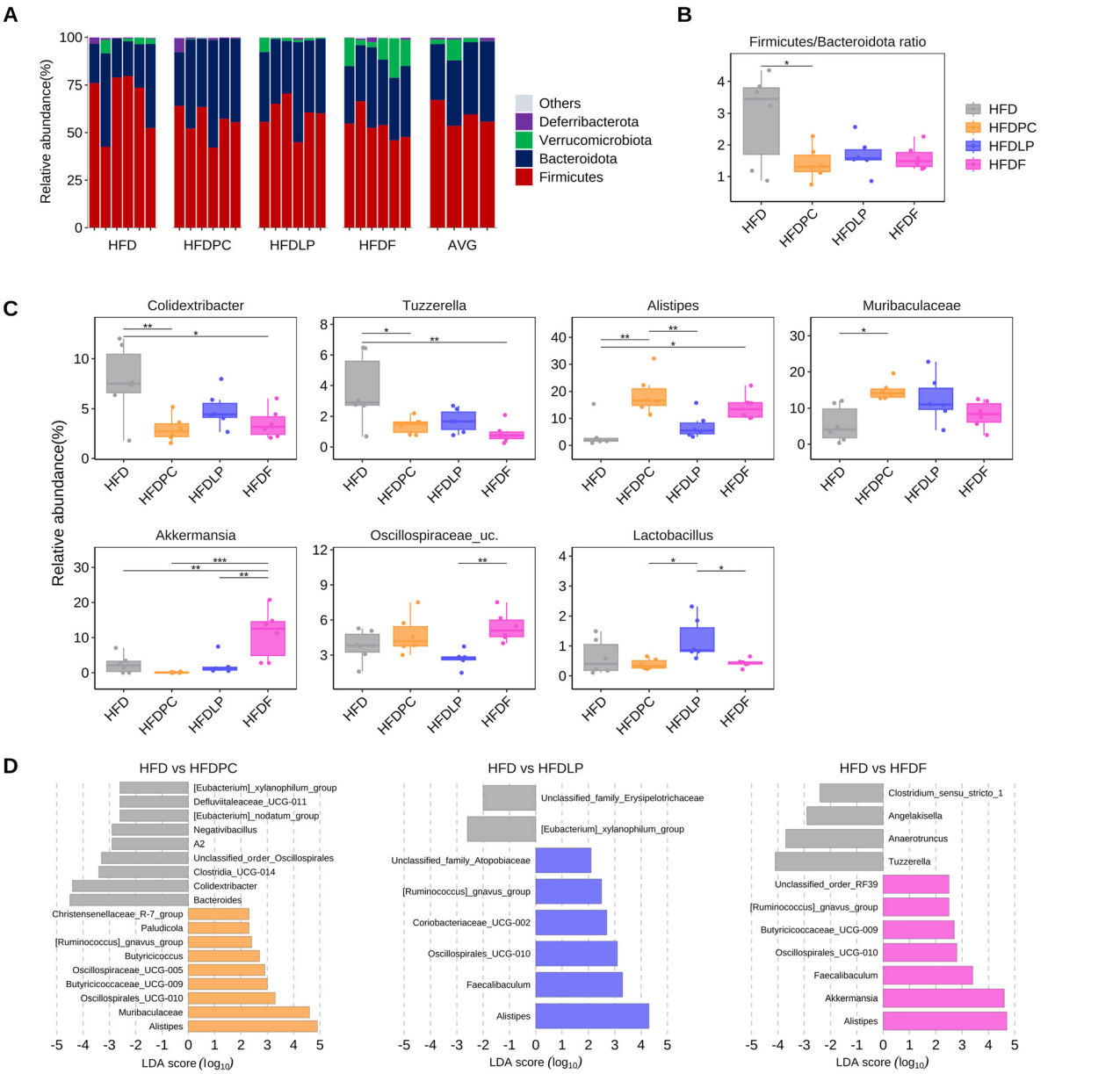

Fig. 8 Effect of the probiotic formulation on the gut microbiota in a high-fat diet-induced obesity mouse model. (A) Taxonomic compositions in the four (HFD, high fat diet; HFDPC, HFD with *Lacticaseibacillus paracasei* BEPC22; HFDLP, HFD with *Lactiplantibacillus plantarum* BELP53; HFDF, HFD with the combination of two strains) groups and the AVG (average) of each group at the phylum level. (B) Significant differences in the Firmicutes/Bacteroidota ratio in the four groups. (C) Differences in the microbiota abundance at the genus level. (D) Differing abundance of the bacterial communities between each group determined using LEfSe. Significance is indicated by *$p < 0.05$, **$p < 0.01$, ***$p < 0.001$, and ****$p < 0.0001$ as compared with the HFD group.

Ppar-γ in the liver was lower in the probiotic-treated groups than in the HFD group. Moreover, the HFDF group showed the lowest *Ppar-γ* expression. This result indicated that the administration of BEPC22 and BELP53 hindered *Ppar-γ* expression in the liver, which consequently inhibited fatty acid synthesis and decreased subcutaneous and abdominal fat weights.

The gut microbiome is associated with obesity and related metabolic disorders, and specific metabolites correlate with the structure of the gut microbiome.[48,49] In the present study, the metabolome and microbiome analyses including the ND group showed a significantly distinct pattern between the ND and HFD groups. The PLS-DA (ESI Fig. 6A†) based on the metabolome data shows a clear separation between the ND and HFD (without and with the probiotic-treated groups) groups. Similarly, microbiome data showed a distinguished pattern of ND from HFD with the probiotic groups. Among alpha diversity (ESI Fig. 6B†), the observed features were significantly reduced in the HFD group compared to the ND group, and the alpha diversity in the formulation feeding group (HFDF) was recovered as much as in the ND group. In

the beta diversity (ESI Fig. 6C†) analysis, the ND and HFD groups showed a significant difference, and the probiotic-treated groups were not close to the ND group, but the HFDF group was the closest to the ND group. The microbiome results indicate that the HFDF group is most similar to the ND group among the high fat diet-fed groups. In the faecal microbiome analysis excluding the ND group, the abundance of *Colidextribacter* and *Tuzzerella* decreased, whereas that of *Alistipes*, *Akkermansia*, and *Muribaculaceae* increased in the probiotic-fed groups compared with the HFD group. Previous studies have reported that the abundance of *Colidextribacter* increases in individuals with obesity, whereas the abundance of *Akkermansia*, a beneficial bacterium, increases in healthy lean individuals, but is depleted in those with obesity and metabolic diseases.[50,51] *Alistipes* is also more prevalent in healthy lean individuals and less prevalent in individuals with obesity, and these strains produce small amounts of SCFAs, which can inhibit Ppar-γ expression and promote fat oxidation.[52] Furthermore, it was reported that *Alistipes* is capable of synthesizing membrane building blocks by utilizing medium- and long-chain fatty acids within the gut.[53] However, our results represented reduction of some phospholipids with significant correlation with *Alistipes*. We guess the inconsistent result may be due to the different substrate specificity of the acyl-acyl carrier protein (ACP) synthetase in *Alistipes*, which form phospholipids.

We observed changes in lipids and specific metabolites in the faecal and plasma samples and correlated these changes with certain microbiomes. The HFDF group showed a different lipid composition in the faeces than the other groups. We assumed that the administered probiotics affected the lipid pool by modulating the gut microbiota, such as *Faecalibaculum*, *Ruminococcus*, *Coriobacteriaceae*, and *Atopobiaceae*. Among the identified lipids, Cer(d18 : 0/0 : 0) significantly correlated with body weight gain, fat weight, and *Ppar-α* mRNA expression in the adipose tissue, which is consistent with the results of a previous research.[54] Additionally, as mentioned in previous research, an elevated level of *Faecalibaculum* in obesity mouse models was associated with weight loss.[55,56] Our study showed that the level of PG(18 : 2/0 : 0) is increased along with the *Faecalibaculum* abundance in the faeces. As a result, we assumed that *Alistipes* and *Faecalibaculum* are important changers who change the gut lipid profile, potentially contributing to reduced weight gain.

In addition, the amount of pantothenic acid, a key precursor of coenzyme A, significantly increased in the faeces of the HFDF group and was positively correlated with *Akkermansia*, *Coriobacteriaceae*, and *Atopobiaceae* (ESI Fig. 6†).

Furthermore, among the metabolites detected in the plasma, hippuric acid and indolelactic acid had comparatively higher levels in the HFDF group than in the other groups and were significantly correlated with anti-obesity indicators, such as fat weight and *Ppar-α* expression, in the epididymal adipose tissue.

Hippuric acid, possessing the protective effect against obesity, was relatively higher in the plasma of HFDF mice.[57,58] Most studies revealed that the hippuric acid is originated from polyphenols in fruits and whole grains.[58] However, in our study, we observed hippuric acid even though polyphenols were not supplied. Thus, we assumed that the hippuric acid might be produced from phenylalanine by the gut microbiota, and then, conjugated with glycine in the liver.[59] Indole derivatives, which are tryptophan metabolites produced by the gut microbiota, play crucial roles in influencing gut homeostasis and immune responses. They are transported through the bloodstream to regulate lipid metabolism in the liver. Changes in dietary patterns can lead to metabolic disorders owing to gut dysbiosis, which can significantly affect indole metabolism.[60] In the present study, indole-3-propionic acid and indolelactic acid were detected in the plasma of the HFD-fed mice, but only indolelactic acid showed a significantly higher level in the HFDF group, with a notable correlation with *Coriobacteriaceae* and *Faecalibaculum* (ESI Fig. 7†). Previous studies have shown that the indolelactic acid produced by *L. plantarum* modulates the gut environment, thus promoting the proliferation of *Faecalibacterium* and *Bifidobacterium*.[61]

Taken together, probiotic formulations with BEPC22 and BELP53 showed an anti-obesity effect not only by perturbation of lipid metabolism, but with assistance of anti-obesity metabolites such as hippuric acid and indole derivatives which might be synthesized by the changed gut microbiome. We guess that the altered gut microbial community was more capable of metabolizing aromatic amino acids (*e.g.* tryptophan and tyrosine) that eventually produced host beneficial metabolites (*e.g.* hippuric acid and indole derivatives). Therefore, we think it is imperative to construct gut microbial communities by harmonizing some microbes involved in lipid metabolism and other microorganisms responsible for producing metabolites with an anti-obesity effect for better efficacy. Even we observed an anti-obesity effect of the formulation in this study; the interaction of the abovementioned metabolites with specific colonic bacteria and the mechanisms underlying weight gain are needed to be understood in further studies.

Conclusions

The two-strain formulation effectively alleviated HFD-induced obesity in mice. The competitive lipid and carbohydrate metabolic characteristics of the two strains, which are expected to ameliorate obesity, may have resulted in changes in body weight, body fat mass, gut microbiota, and lipid profiles. Specifically, the administration of the two strains modulated the F/B ratio of the gut bacteria, which consequently decreased the abundance of certain genera associated with obesity. Furthermore, it increased blood indolelactic acid levels, which decreased during metabolic abnormalities, and enhanced intestinal lipid excretion. While our study successfully identified microbial changes and their corresponding metabolomic correlates, further investigation at the molecular pathway level is imperative to gain a deeper understanding of the mechanisms by which these two strains ameliorate obesity. Further

research in this field will contribute to the development of obesity prevention strategies.

Data availability

All data underlying the results are available as part of the article and no additional source data are required.

Author contributions

Conceptualisation: S. J. Kim and K.-J. Sin; data curation: N.-R. Lee, E.-C. Chung, J. W. Bae, T.-J. Kwon and N. W. Hwang; formal analysis: N.-R. Lee, S.-H. Soung, H.-J. Tak, T.-J. Kwon, J.-Y. Choi, Y.-E. Lee and N. W. Hwang; investigation: N.-R. Lee, J. S. Lee, E.-C. Chung, T.-J. Kwon, S.-H. Soung and H.-J. Tak; methodology: N.-R. Lee, J. S. Lee and T.-J. Kwon; project administration: S. J. Kim, K.-J. Sin, J. S. Lee and K. S. Kim; resources: E.-C. Chung; software: J. W. Bae; supervision: C. H. Lee; visualization: N.-R. Lee, T.-J. Kwon and J. W. Bae; writing – original draft: N.-R. Lee, E.-C. Chung, J. W. Bae and T.-J. Kwon; and writing – review and editing: S.J. Kim and K.-J. Sin.

Conflicts of interest

There are no conflicts to declare.

Acknowledgements

This work was supported by the Ministry of Trade, Industry and Energy (MOTIE) and the Korea Evaluation Institute of Industrial Technology (KEIT) through the Research and Development Project for the Advanced Technology Center (ATC+) (Project No. 20009679, NTIS_1415179891).

References

1 M. Blüher, Obesity: global epidemiology and pathogenesis, *Nat. Rev. Endocrinol.*, 2019, **15**, 288–298.
2 H. M. Timmerman, C. J. Koning, L. Mulder, F. M. Rombouts and A. C. Beynen, Monostrain, multistrain and multispecies probiotics—a comparison of functionality and efficacy, *Int. J. Food Microbiol.*, 2004, **96**, 219–233.
3 M. Miyoshi, A. Ogawa, S. Higurashi and Y. Kadooka, Anti-obesity effect of Lactobacillus gasseri SBT2055 accompanied by inhibition of pro-inflammatory gene expression in the visceral adipose tissue in diet-induced obese mice, *Eur. J. Nutr.*, 2014, **53**, 599–606.
4 W. H. Jeung, J. J. Shim, S. W. Woo, J. H. Sim and J. L. Lee, Lactobacillus curvatus HY7601 and Lactobacillus plantarum KY1032 Cell Extracts Inhibit Adipogenesis in 3T3-L1 and HepG2 Cells, *J. Med. Food*, 2018, **21**, 876–886.
5 Y. Kang, X. Kang, H. Yang, H. Liu, X. Yang, Q. Liu, H. Tian, Y. Xue, P. Ren, X. Kuang, Y. Cai, M. Tong, L. Li and W. Fan, Lactobacillus acidophilus ameliorates obesity in mice through modulation of gut microbiota dysbiosis and intestinal permeability, *Pharmacol. Res.*, 2022, **175**, 106020.
6 S. Adamberg, I. Sumeri, R. Uusna, P. Ambalam, K. Kiran Kondepudi, K. Adamberg, T. Wadström, Å. Ljungh, T. Wadströ and A. Ljungh, Survival and synergistic growth of mixed cultures of bifidobacteria and lactobacilli combined with prebiotic oligosaccharides in a gastrointestinal tract simulator, *Microb. Ecol. Health Dis.*, 2014, **25**, 23062.
7 L. V. McFarland, Efficacy of single-strain probiotics versus multi-strain mixtures: systematic review of strain and disease specificity, *Dig. Dis Sci.*, 2021, **66**, 694–704.
8 P. D. Cani and N. M. Delzenne, Gut microflora as a target for energy and metabolic homeostasis, *Curr. Opin. Clin. Nutr. Metab. Care*, 2007, **10**, 729–734.
9 E. M. Hamad, M. Sato, K. Uzu, T. Yoshida, S. Higashi, H. Kawakami, Y. Kadooka, H. Matsuyama, I. A. Abd El-Gawad and K. Imaizumi, Milk fermented by Lactobacillus gasseri SBT2055 influences adipocyte size via inhibition of dietary fat absorption in Zucker rats, *Br. J. Nutr.*, 2008, **101**, 716–724.
10 G. Karimi, M. R. Sabran, R. Jamaluddin, K. Parvaneh, N. Mohtarrudin, Z. Ahmad, H. Khazaai and A. Khodavandi, The anti-obesity effects of Lactobacillus casei strain Shirota versus Orlistat on high fat diet-induced obese rats, *Food Nutr. Res.*, 2015, **59**, 29273.
11 Z. Cheng, L. Zhang, L. Yang and H. Chu, The critical role of gut microbiota in obesity, *Front. Endocrinol.*, 2022, **13**(1025706).
12 M. Million, E. Angelakis, M. Maraninchi, M. Henry, R. Giorgi, R. Valero, B. Vialettes and D. Raoult, Correlation between body mass index and gut concentrations of Lactobacillus reuteri, Bifidobacterium animalis, Methanobrevibacter smithii and Escherichia coli, *Int. J. Obes.*, 2013, **37**, 1460–1466.
13 A. Andoh, A. Nishida, K. Takahashi, O. Inatomi, H. Imaeda, S. Bamba, K. Kito, M. Sugimoto and T. Kobayashi, Comparison of the gut microbial community between obese and lean peoples using 16S gene sequencing in a Japanese population, *J. Clin. Biochem. Nutr.*, 2016, **59**, 65–70.
14 S. M. Murga-Garrido, Y. C. Orbe-Orihuela, C. E. Díaz-Benítez, A. C. Castañeda-Márquez, F. Cornejo-Granados, A. Ochoa-Leyva, A. Sanchez-Flores, M. Cruz, A. I. Burguete-García and A. Lagunas-Martínez, Alterations of the gut microbiome associated to methane metabolism in Mexican children with obesity, *Children*, 2022, **9**, 148.
15 A. Koliada, G. Syzenko, V. Moseiko, L. Budovska, K. Puchkov, V. Perederiy, Y. Gavalko, A. Dorofeyev, M. Romanenko, S. Tkach, L. Sineok, O. Lushchak and A. Vaiserman, Association between body mass index and Firmicutes/Bacteroidetes ratio in an adult Ukrainian population, *BMC Microbiol.*, 2017, **17**, 1–6.
16 P. Thiennimitr, S. Yasom, W. Tunapong, T. Chunchai, K. Wanchai, A. Pongchaidecha, A. Lungkaphin, S. Sirilun,

C. Chaiyasut, N. Chattipakorn and S. C. Chattipakorn, Lactobacillus paracasei HII01, xylooligosaccharides, and synbiotics reduce gut disturbance in obese rats, *Nutrition*, 2018, **54**, 40–47.

17 J. Geng, Q. Ni, W. Sun, L. Li and X. Feng, The links between gut microbiota and obesity and obesity related diseases, *Biomed. Pharmacother.*, 2022, **147**, 112678.

18 S. Y. Son, S. Lee, D. Singh, N.-R. Lee, D. Y. Lee and C. H. Lee, Comprehensive secondary metabolite profiling toward delineating the solid and submerged-state fermentation of Aspergillus oryzae KCCM 12698, *Front. Microbiol.*, 2018, **9**, 1076.

19 Y. H. Lee, N.-R. Lee and C. H. Lee, Comprehensive metabolite profiling of four different beans fermented by Aspergillus oryzae, *Molecules*, 2022, **27**, 7917.

20 L. Han, Y. Kimura and H. Okuda, Reduction in fat storage during chitin-chitosan treatment in mice fed a high-fat diet, *Int. J. Obes.*, 1999, **23**, 174–179.

21 N.-J. Song, H.-J. Yoon, K. H. Kim, S.-R. Jung, W.-S. Jang, C.-R. Seo, Y. M. Lee, D.-H. Kweon, J.-W. Hong, J.-S. Lee, K.-M. Park, K. R. Lee and K. W. Park, Butein is a novel anti-adipogenic compound, *J. Lipid Res.*, 2013, **54**, 1385–1396.

22 E. Bolyen, J. R. Rideout, M. R. Dillon, N. A. Bokulich, C. C. Abnet, G. A. Al-Ghalith, H. Alexander, E. J. Alm, M. Arumugam, F. Asnicar, Y. Bai, J. E. Bisanz, K. Bittinger, A. Brejnrod, C. J. Brislawn, C. T. Brown, B. J. Callahan, A. M. Caraballo-Rodríguez, J. Chase, E. K. Cope, R. Da Silva, C. Diener, P. C. Dorrestein, G. M. Douglas, D. M. Durall, C. Duvallet, C. F. Edwardson, M. Ernst, M. Estaki, J. Fouquier, J. M. Gauglitz, S. M. Gibbons, D. L. Gibson, A. Gonzalez, K. Gorlick, J. Guo, B. Hillmann, S. Holmes, H. Holste, C. Huttenhower, G. A. Huttley, S. Janssen, A. K. Jarmusch, L. Jiang, B. D. Kaehler, K. Bin Kang, C. R. Keefe, P. Keim, S. T. Kelley, D. Knights, I. Koester, T. Kosciolek, J. Kreps, M. G. I. Langille, J. Lee, R. Ley, Y.-X. Liu, E. Loftfield, C. Lozupone, M. Maher, C. Marotz, B. D. Martin, D. McDonald, L. J. McIver, A. V. Melnik, J. L. Metcalf, S. C. Morgan, J. T. Morton, A. T. Naimey, J. A. Navas-Molina, L. F. Nothias, S. B. Orchanian, T. Pearson, S. L. Peoples, D. Petras, M. L. Preuss, E. Pruesse, L. B. Rasmussen, A. Rivers, M. S. Robeson II, P. Rosenthal, N. Segata, M. Shaffer, A. Shiffer, R. Sinha, S. J. Song, J. R. Spear, A. D. Swafford, L. R. Thompson, P. J. Torres, P. Trinh, A. Tripathi, P. J. Turnbaugh, S. Ul-Hasan, J. J. J. Van der Hooft, F. Vargas, Y. Vázquez-Baeza, E. Vogtmann, M. von Hippel, W. Walters, Y. Wan, M. Wang, J. Warren, K. C. Weber, C. H. D. Williamson, A. D. Willis, Z. Z. Xu, J. R. Zaneveld, Y. Zhang, Q. Zhu, R. Knight and J. G. Caporaso, Reproducible, interactive, scalable and extensible microbiome data science using QIIME 2, *Nat. Biotechnol.*, 2019, **37**, 852–857.

23 A. Amir, D. McDonald, J. A. Navas-Molina, E. Kopylova, J. T. Morton, Z. Zech Xu, E. P. Kightley, L. R. Thompson, E. R. Hyde, A. Gonzalez and R. Knight, Deblur Rapidly Resolves Single-Nucleotide Community Sequence Patterns, *mSystems*, 2017, **2**, e00191–e00116.

24 K. Katoh, K. Misawa, K. Kuma and T. Miyata, MAFFT: a novel method for rapid multiple sequence alignment based on fast Fourier transform, *Nucleic Acids Res.*, 2002, **30**, 3059–3066.

25 D. P. Faith, Conservation evaluation and phylogenetic diversity, *Biol. Conserv.*, 1992, **61**, 1–10.

26 C. A. Lozupone, M. Hamady, S. T. Kelley and R. Knight, Quantitative and qualitative β diversity measures lead to different insights into factors that structure microbial communities, *Appl. Environ. Microbiol.*, 2007, **73**, 1576–1585.

27 C. Lozupone and R. Knight, UniFrac: A new phylogenetic method for comparing microbial communities, *Appl. Environ. Microbiol.*, 2005, **71**, 8228–8235.

28 N. A. Bokulich, B. D. Kaehler, J. R. Rideout, M. Dillon, E. Bolyen, R. Knight, G. A. Huttley and J. Gregory Caporaso, Optimizing taxonomic classification of marker-gene amplicon sequences with QIIME 2's q2-feature-classifier plugin, *Microbiome*, 2018, **6**, 1–17.

29 C. Quast, E. Pruesse, P. Yilmaz, J. Gerken, T. Schweer, P. Yarza, J. Peplies and F. O. Glöckner, The SILVA ribosomal RNA gene database project: improved data processing and web-based tools, *Nucleic Acids Res.*, 2012, **41**, D590–D596.

30 M. J. Anderson, A new method for non–parametric multivariate analysis of variance, *Aust. Ecol.*, 2008, **26**, 32–46.

31 N. Segata, J. Izard, L. Waldron, D. Gevers, L. Miropolsky, W. S. Garrett and C. Huttenhower, Metagenomic biomarker discovery and explanation, *Genome Biol.*, 2011, **12**, 1–18.

32 M. Hirose, T. Ando, R. Shofiqur, K. Umeda, Y. Kodama, S. Van Nguyen, T. Goto, M. Shimada and S. Nagaoka, Anti-obesity activity of hen egg anti-lipase immunoglobulin yolk, a novel pancreatic lipase inhibitor, *Nutr. Metab.*, 2013, **10**, 1–6.

33 J. K. Sethi and A. J. Vidal-Puig, Adipose tissue function and plasticity orchestrate nutritional adaptation, *J. Lipid Res.*, 2007, **48**, 1253–1262.

34 S. J. Kim, S.-I. Choi, M. Jang, Y. Jeong, C.-H. Kang and G.-H. Kim, Anti-adipogenic effect of Lactobacillus fermentum MG4231 and MG4244 through AMPK pathway in 3T3-L1 preadipocytes, *Food Sci. Biotechnol.*, 2020, **29**, 1541–1551.

35 Y.-C. Lin, Y.-T. Chen, K.-Y. Li and M.-J. Chen, Investigating the mechanistic differences of obesity-inducing Lactobacillus kefiranofaciens M1 and anti-obesity Lactobacillus mali APS1 by microbolomics and metabolomics, *Front. Microbiol.*, 2020, **11**, 1454.

36 E. J. Culp and A. L. Goodman, Cross-feeding in the gut microbiome: Ecology and mechanisms, *Cell Host Microbe*, 2023, **31**, 485–499.

37 C. Weyer, J. E. Foley, C. Bogardus, P. A. Tataranni and R. E. Pratley, Enlarged subcutaneous abdominal adipocyte size, but not obesity itself, predicts Type II diabetes independent of insulin resistance, *Diabetologia*, 2000, **43**, 1498–1506.

38 R. V. Considine, M. K. Sinha, M. L. Heiman, A. Kriauciunas, T. W. Stephens, M. R. Nyce, J. P. Ohannesian, C. C. Marco, L. J. McKee, T. L. Bauer and J. F. Caro, Serum Immunoreactive-Leptin Concentrations in

Normal-Weight and Obese Humans, *N. Engl. J. Med.*, 1996, **334**, 292–295.

39 F. Lönnqvist, P. Arner, L. Nordfors and M. Schalling, Overexpression of the obese (ob) gene in adipose tissue of human obese subjects, *Nat. Med.*, 1995, **1**, 950–953.

40 B. S. Hamilton, D. Paglia, A. Y. M. Kwan and M. Deitel, Increased obese mRNA expression in omental fat cells from massively obese humans, *Nat. Med.*, 1995, **1**, 953–956.

41 P. J. Scarpace, M. Nicolson and M. Matheny, UCP2, UCP3 and leptin gene expression: modulation by food restriction and leptin, *J. Endocrinol.*, 1998, **159**, 349–357.

42 M. Alivand, B. Alipour, S. Moradi, Y. Khaje-Bishak and M. Alipour, The review of the relationship between UCP2 and obesity: Focusing on inflammatory-obesity, *New insight in Obesity: Genetics and Beyond*, 2021, **5**, 1–13.

43 I. Emilia, G. C. Farrell, G. Robertson, P. Hall, R. Kirsch and I. Leclercq, Central role of PPARα-dependent hepatic lipid turnover in dietary steatohepatitis in mice, *Hepatology*, 2003, **38**, 123–132.

44 W. J. Lee, M. Kim, H.-S. Park, H. S. Kim, M. J. Jeon, K. S. Oh, E. H. Koh, J. C. Won, M.-S. Kim, G. T. Oh, M. Yoon, K.-U. Lee and J.-Y. Park, AMPK activation increases fatty acid oxidation in skeletal muscle by activating PPARα and PGC-1, *Biochem. Biophys. Res. Commun.*, 2006, **1**, 291–295.

45 M. Vázquez, N. Roglans, Á. Cabrero, C. Rodríguez, T. Adzet, M. Alegret, R. M. Sánchez and J. C. Laguna, Bezafibrate induces acyl-CoA oxidase mRNA levels and fatty acid peroxisomal β-oxidation in rat white adipose tissue, *Mol. Cell. Biochem.*, 2001, **216**, 71–78.

46 A. Cabrero, M. Alegret, R. M. Sánchez, T. Adzet, J. C. Laguna and M. Vázquez, Bezafibrate reduces mRNA levels of adipocyte markers and increases fatty acid oxidation in primary culture of adipocytes, *Diabetes*, 2001, **50**, 1883–1890.

47 A. P. L. Jensen-Urstad and C. F. Semenkovich, Fatty acid synthase and liver triglyceride metabolism: housekeeper or messenger?, *Biochim. Biophys. Acta, Bioenerg.*, 2012, **1821**, 747–753.

48 H. S. Ejtahed, A. R. Soroush, P. Angoorani, B. Larijani and S. Hasani-Ranjbar, Gut Microbiota as a Target in the Pathogenesis of Metabolic Disorders: A New Approach to Novel Therapeutic Agents, *Horm. Metab. Res.*, 2016, **48**, 349–358.

49 G. Sharon, N. Garg, J. Debelius, R. Knight, P. C. Dorrestein and S. K. Mazmanian, Specialized metabolites from the microbiome in health and disease, *Cell Metab.*, 2014, **20**, 719–730.

50 Z. Yu, X. F. Yu, G. Kerem and P. G. Ren, Perturbation on gut microbiota impedes the onset of obesity in high fat diet-induced mice, *Front. Endocrinol.*, 2022, **13**, 795371.

51 G. den Besten, A. Bleeker, A. Gerding, K. van Eunen, R. Havinga, T. H. van Dijk, M. H. Oosterveer, J. W. Jonker, A. K. Groen, D.-J. Reijngoud and B. M. Bakker, Short-chain fatty acids protect against high-fat diet–induced obesity via a PPARγ-dependent switch from lipogenesis to fat oxidation, *Diabetes*, 2015, **64**, 2398–2408.

52 Z. Xu, W. Jiang, W. Huang, Y. Lin, F. K. L. Chan and S. C. Ng, Gut microbiota in patients with obesity and metabolic disorders—a systematic review, *Genes Nutr.*, 2022, **17**, 1–18.

53 C. D. Radka, M. W. Frank, C. O. Rock and J. Yao, Fatty acid activation and utilization by Alistipes finegoldii, a representative Bacteroidetes resident of the human gut microbiome, *Mol. Microbiol.*, 2020, **113**, 807–825.

54 H. Fang, Y. Cao, J. Zhang, X. Wang, M. Li, Z. Hong, Z. Wu and M. Fang, Lipidome remodeling activities of DPA-EA in palmitic acid-stimulated HepG2 cells and the in vivo anti-obesity effect of the DPA-EA and DHA-EA mixture prepared from algae oil, *Front. Pharmacol.*, 2023, **14**, 1146276.

55 S. Wang, M. Huang, X. You, J. Zhao, L. Chen, L. Wang, Y. Luo and Y. Chen, Gut microbiota mediates the anti-obesity effect of calorie restriction in mice, *Sci. Rep.*, 2018, **8**, 13037.

56 G. H. Baek, K. M. Yoo, S.-Y. Kim, D. H. Lee, H. Chung, S.-C. Jung, S.-K. Park and J.-S. Kim, Collagen Peptide Exerts an Anti-Obesity Effect by Influencing the Firmicutes/Bacteroidetes Ratio in the Gut, *Nutrients*, 2023, **15**, 2610.

57 K. M. Pruss, H. Chen, Y. Liu, W. Van Treuren, S. K. Higginbottom, J. B. Jarman, C. R. Fischer, J. Mak, B. Wong, T. M. Cowan, M. A. Fischbach, J. L. Sonnenburg and D. Dodd, Host-microbe co-metabolism via MCAD generates circulating metabolites including hippuric acid, *Nat. Commun.*, 2023, **14**, 512.

58 T. Pallister, M. A. Jackson, T. C. Martin, C. A. Glastonbury, A. Jennings, M. Beaumont, R. P. Mohney, K. S. Small, A. MacGregor, C. J. Steves, A. Cassidy, T. D. Spector, C. Menni and A. M. Valdes, Untangling the relationship between diet and visceral fat mass through blood metabolomics and gut microbiome profiling, *Int. J. Obes.*, 2017, **41**, 1106–1113.

59 A. Ticinesi, A. Guerra, A. Nouvenne, T. Meschi and S. Maggi, Disentangling the Complexity of Nutrition, Frailty and Gut Microbial Pathways during Aging: A Focus on Hippuric Acid, *Nutrients*, 2023, **15**, 1138.

60 X. Li, B. Zhang, Y. Hu and Y. Zhao, New Insights Into Gut-Bacteria-Derived Indole and Its Derivatives in Intestinal and Liver Diseases, *Front. Pharmacol.*, 2021, **12**, 769501.

61 Q. Zhou, Z. Xie, D. Wu, L. Liu, Y. Shi, P. Li and Q. Gu, The Effect of Indole-3-Lactic Acid from Lactiplantibacillus plantarum ZJ316 on Human Intestinal Microbiota In Vitro, *Foods*, 2022, **11**, 3302.

